

Doping dependence of the optical properties of $\text{Ba}_{1-x}\text{K}_x\text{BiO}_3$

A. V. Puchkov and T. Timusk

Department of Physics and Astronomy, McMaster University, Hamilton, Ontario, Canada L8S 4M1

M. A. Karlow and S. L. Cooper

Department of Physics and Material Research Laboratory, University of Illinois at Urbana-Champaign, 104 South Goodwin Avenue, Urbana, Illinois 61801

P. D. Han and D. A. Payne

Department of Material Science and Engineering and Material Research Laboratory, University of Illinois at Urbana-Champaign, 104 South Goodwin Avenue, Urbana, Illinois 61801

(Received 10 January 1996)

We analyze the doping dependence of the optical conductivity of the $\text{Ba}_{1-x}\text{K}_x\text{BiO}_3$ (BKBO) system in the full doping range from $x=0$ to $x=0.46$. We have used the results of our reflectivity and ellipsometric measurements at $x=0.31, 0.38, 0.4, 0.46$, as well as the results obtained by other experimental groups at different doping levels, to analyze the doping dependence of the spectral weight distribution. At the insulator-metal transition boundary we observe the appearance of a Drude-like free-carrier peak in the optical conductivity. In the metallic phase, we have performed measurements in the normal as well as the superconducting state. The data show that BKBO becomes a better metal with increasing x in the metallic regime due to a decrease in the scattering rate of the metallic charge carriers, while the density of the mobile (Drude) charge carriers does not significantly change with doping. The London penetration depth λ_L is also found to be almost doping (and T_c) independent while the superconducting gap scales with T_c as $2\Delta_s/k_bT_c = 4.2 \pm 0.3$.
[S0163-1829(96)07434-6]

In the last two years several experimental reports regarding the insulator-metal (IM) transition and the evolution of optical properties as a function of doping level x in $\text{Ba}_{1-x}\text{K}_x\text{BiO}_3$ (BKBO) have been published.^{1,2} In this paper we use the large amount of experimental material accumulated to date to discuss the properties of the BKBO system in the nonmetallic phase using sum-rule analysis. In the metallic phase, optical studies of the doping dependence have previously been done, to our knowledge, only at room temperature and at relatively high photon energies. We fill this gap by performing reflectivity and ellipsometric measurements in a combined range of $30\text{--}50\,000\text{ cm}^{-1}$ on three superconducting BKBO single crystals ($T_c=21, 28, \text{ and } 31\text{ K}$).

The BKBO single crystals used in this study were grown by an electrochemical method.³ The lattice parameters were measured by x-ray diffraction using a Rigaku *D*-max diffractometer ($\text{Cu } K\alpha, \lambda = 1.5405\text{ \AA}$). After the optical measurements, the crystals were ground into powder and x-ray diffraction measurements were carried out on the powdered sample intermixed with high-purity Ge powder which acted as an internal x-ray standard. The lattice parameters were refined by a least-squares fit routine with calibration against Ge. The potassium concentration x was estimated from the linear relationship between the pseudocubic lattice parameter a and potassium concentration x .⁴

The optical experiments were performed at temperatures ranging from $T_c/3$ to room temperature. We have used Kramers-Kronig (KK) analysis of reflectivity, supplemented by results of ellipsometric measurements, to obtain the complex optical conductivity $\sigma(\omega)$ in the normal and the superconducting states.

The undoped material BaBiO_3 has one electron per unit cell and therefore should be a metal with a half-filled conduction band. However, it is in fact an insulator. Experimentally observed frozen breathing-type lattice distortions^{4,5} led to a suggestion that BaBiO_3 is made insulating by a charge-density-wave (CDW) instability that opens a gap on the Fermi level, splitting the conduction band into two subbands: a filled lower CDW subband and an empty upper CDW subband.⁶ However, this model leaves some questions unanswered. In particular, there is no clear understanding of the nature of the midinfrared (MIR) absorption peak at nonzero doping levels. Also, results of band structure calculations indicate that the observed lattice distortions are not sufficient to produce a gap in the electronic density of states.⁷ Another model, advanced to explain the insulating nature of BKBO at low doping levels, involves real-space pairing of electrons in pairs strongly localized on the Bi sites: small bipolarons.⁸ There is a number of experimental results that favor the bipolaronic model, including those of Raman scattering,⁹ infrared reflectivity,¹⁰ and high-resolution electron energy loss spectroscopy.¹¹ Several recent reports on the doping dependence of optical properties of the BKBO system^{1,2,10} allow us to examine this problem once again on a more quantitative level.

We will first concentrate on the properties of the BKBO system in the nonmetallic phase and at the IM transition boundary. The optical conductivity of insulating BKBO shows a well-resolved MIR peak with a maximum at $\hbar\omega_{\text{max}}$, equal to 2 eV in the undoped BaBiO_3 .^{1,2,12} As the doping level x increases, the position of the maximum of the MIR absorption shifts gradually to lower energies.

However, this contribution to the optical conductivity can be observed at all doping levels. The IM transition occurs at $x_c \approx 0.33-0.35$ and is illustrated in Fig. 1, where optical conductivity is shown for the nonmetallic sample with $x=0.31$ and for the metallic sample with $x=0.38$. The difference between the two curves is qualitative: While in the metallic sample $\hbar\omega_{\max}$ has collapsed to zero so that no clear maximum can be seen in the MIR absorption band, an additional free-carrier-like narrow ($1/\tau \leq 300 \text{ cm}^{-1}$) absorption band has appeared at low frequency.¹³ This latter absorption component, called hereafter the ‘‘Drude’’ absorption band, is responsible for the metallic properties of this material at doping levels $x > x_c$.

The MIR absorption band in BKBO is well separated from the rest of the interband absorption, allowing us to employ a finite-energy f sum-rule analysis to obtain the plasma frequency associated with the MIR absorption, $\omega_{p\text{MIR}}$. The key requirement that must be satisfied in order for the finite-energy f sum rule to hold is that the absorption in question be sufficiently isolated. In this case the plasma frequency associated with the isolated absorption is calculated as an integral of the real part of the optical conductivity over energies from zero to a cutoff energy $\hbar\omega_0$,¹⁴ which must be chosen to exhaust the oscillator strength of the absorption in question but lie below the rest of the absorption bands. If $\hbar\omega_0$ is extended to infinity, one obtains the conductivity f sum rule where the plasma frequency ω_p is given by the total density of electrons in the material (including inner-shell electrons), $\omega_p^2 = 4\pi n e^2 / m_b$, where n is the density of electrons and m_b is a bare electron mass.

In analogy with the f sum rule we can define an effective density of electrons contributing to the optical transition represented by the MIR band, n_{eff} , by $\omega_{p\text{MIR}}^2 = 4\pi n_{\text{eff}} e^2 / m_b$. On the other hand, the density of electrons, n , can also be determined from the chemical composition using the concentration of Bi ions, $x: n(x) = (1-x)/v_c$, where v_c is the volume per Bi ion. The $n(x)$, calculated this way, is plotted as the straight line in Fig. 2(b). To calculate the straight line, average lattice parameters of the BKBO system were used to obtain v_c . Taking into account the actual changes in the lattice parameters with doping does not change the result significantly: We have used experimentally obtained⁴ lattice parameters to calculate $n(x)$ at several x and the results, shown by the small dots, are very close to the straight line. In an analogy with the case of metals with strong electron-phonon interaction,¹⁵ we define the optical effective mass $m^* = n/n_{\text{eff}}$, or mass enhancement factor $\lambda = m^* - 1$, as a quantity that measures the amount of the conductivity spectral weight moved to energies $\hbar\omega > \hbar\omega_0$ through the optical transitions other than those represented by the MIR absorption band. If $\hbar\omega_0$ is large enough so that *all* possible optical transition processes are taken into account, the optical effective mass is equal to the bare electron mass $m^* = 1$ and the oscillator strength is determined only by the density of electrons, n . Filled core electron bands may give their own correction to the effective mass value due to the Pauli principle. This correction is, however, estimated to increase the valence and conduction electron oscillator strength by only about 10–20% (Ref. 14) and will therefore be neglected in further discussions.

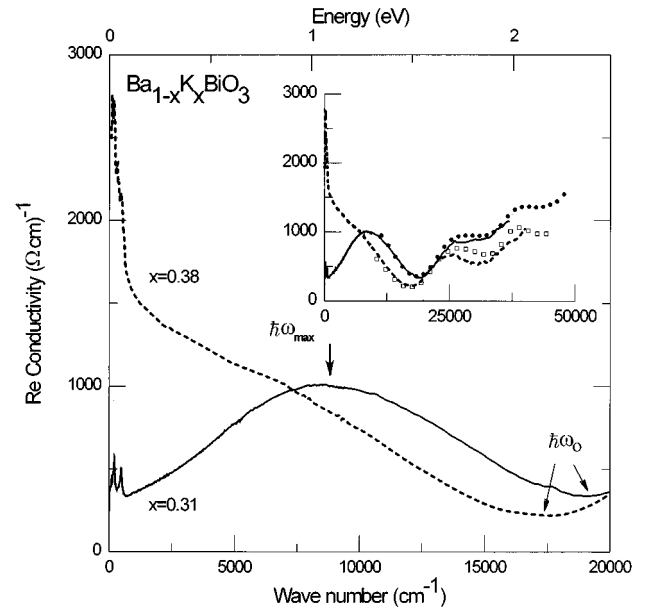


FIG. 1. The optical conductivity of $\text{Ba}_{1-x}\text{K}_x\text{BiO}_3$ just below and just above the insulator-metal transition. The characteristic energies $\hbar\omega_{\max}$ and $\hbar\omega_0$, used in the text, are shown. The inset: the lines represent the real part of the optical conductivity obtained from the KK analysis of reflectivity spectra. The symbols show results of ellipsometric measurements.

We have used $\sigma_1(\omega)$ obtained by different groups on $\text{Ba}_{1-x}\text{K}_x\text{BiO}_3$ at different doping levels to obtain the doping dependence of the oscillator strength of the MIR absorption peak, performing integration of $\sigma_1(\omega)$ as described above. The typical choice of the cutoff frequency is shown in Fig. 1 while the results of our integration are presented in Fig. 2(b). We note that the Drude mobile electrons at $x > x_c$ have a relatively small oscillator strength (about 6% of the MIR) so that the results presented in Fig. 2(b) effectively represent the oscillator strength of the MIR electrons even for the metallic samples. For the metallic samples we have used the loss-function method¹⁶ (with the high-frequency dielectric constant taken from our ellipsometric results) as an alternative to the sum-rule method. The results obtained from the loss function analysis are plotted as open circles.

In this kind of calculation a high degree of accuracy in measuring the absolute value of optical conductivity is obviously very important. Therefore for the heavily doped insulating as well as the metallic samples, where both low- and high-frequency parts of the optical conductivity spectrum contain significant spectral weight, a combination of ellipsometric (above 1 eV) and reflectivity (from $25 \text{ cm}^{-1} = 3.1 \text{ meV}$) results have been used. The nearly perfect agreement between the ellipsometric results, which give dielectric constants above 1 eV directly, and $\sigma_1(\omega)$ obtained from KK analysis of reflectivity data, is shown in the inset of Fig. 1. Spectral weight values obtained from results of different experimental groups at different doping levels are consistent with each other, giving a smooth doping dependence. A measure of the inconsistency is given by the mismatch of the two oscillator strength values at $x=0$ obtained from the results of two different groups that used different optical methods on thin films and single crystals. The inconsistency is about

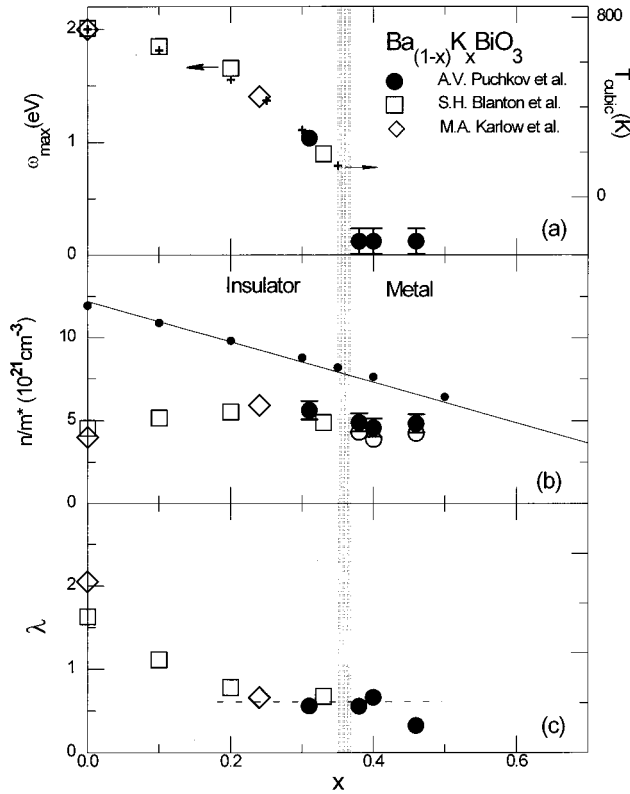


FIG. 2. (a) Large symbols: the doping dependence of the peak energy of the MIR absorption band. Crosses: the doping dependence of temperature of structural transition into the high-temperature cubic phase, T_{cubic} , plotted as described in the text. (b) Large symbols: the doping dependence of the spectral weight of the MIR absorption band obtained as described in the text. The straight line shows the doping dependence of the spectral weight as expected from the chemical composition. The small dots near the straight line were obtained using the actual lattice parameters. (c) The doping dependence of the factor $\lambda(x)$, obtained using results shown in panel (b).

25% and can possibly be due to an error in choosing a high-frequency reflectivity approximation in Ref. 2, where $\sigma_1(\omega)$ was obtained by KK analysis of reflectivity. Ellipsometric measurements give dielectric constants directly in the energy range of the MIR absorption at $x=0$ and therefore we consider the value obtained by Karlov *et al.*¹ to be more reliable. Still, 25% can be considered to be our experimental error in evaluating the oscillator strength.

Results for the doping dependence of the oscillator strength $n(x)/m^*(x)$ obtained using sum-rule analysis [large symbols in Fig. 2(b)] are remarkably different from those expected from the chemical composition [straight line in Fig. 2(b)], leading to high values of m^* at low doping levels, with the highest value being that for the undoped BaBiO_3 , $m^*(0) \approx 3$. These high values of m^* mean that there is a high-energy ($\hbar\omega > \hbar\omega_0$) absorption, not included in our integration, that contains a significant part of the spectral weight. Put differently, not all possible optical transitions involving $n(x)$ chemically doped electrons have been included in our integration. The doping dependence of the mass enhancement factor $\lambda(x) = m^*(x) - 1$, obtained from the ratio of $n(x)$ to $n(x)/m^*(x)$, is plotted in Fig. 2(c). The

value of $\lambda(x)/[\lambda(x)+1]$ gives a fraction of the spectral weight contained at high frequencies so that $\lambda(0) \approx 2$ means that in BaBiO_3 about 2/3 of the total spectral weight due to $n(x)$ chemically doped electrons is contained in the high-energy region above $\hbar\omega_0$. The region of fastest change in $\lambda(x)$ with doping is *below* $x=0.2$. At $x > 0.2$ $\lambda(x)$ is almost doping independent and is approximately equal to 0.5; that is, the spectral weight contained in the higher-energy region is only half of that contained in the MIR absorption band. Estimating our error range somewhat pessimistically, we cannot say with certainty whether or not λ is zero at $x=0.46$.

Let us see if the CDW model, where a single gap opens in the spectrum of electronic excitations, can provide an explanation for the observed doping behavior of the spectral weight. The opening of a *single* gap in the middle of an initially half-filled conduction band redistributes electronic density in the energy region covered by the conduction band, creating a filled lower subband and an empty upper subband. As a result a *single* peak appears in the absorption spectrum positioned at the gap energy corresponding to electronic excitations from the lower subband to the empty upper subband. Assuming that no other optical transitions became possible with the opening of the gap—that is, for example, electronic states in both subbands are still well defined so that no incoherent processes such as those involving emission or absorption of a phonon occur—the optical effective mass of the resulting interband absorption peak must still be equal to unity. In other words the opening of a single gap piles up the spectral weight at energies above the gap value, preserving its total integrated value. Therefore, we conclude that the distribution of the spectral weight discussed above cannot be explained by a single gap in a density of states *only*. Optical excitation processes other than direct excitations across the gap are required.

One such possibility to account for the “missing” spectral weight is to assume that it is contained in the absorption bands corresponding to high-order interband excitations (that is, transitions from a lower CDW subband to bands higher than the upper CDW subband in the CDW model, for example). However, high-order interband transitions usually have matrix elements smaller than that for the first interband transition and therefore do not contain a significant part of the spectral weight. Even if for some reason matrix elements of such transitions are unusually large in BKBO so that they account for a considerable amount of the spectral weight (twice that for the lower-to-upper subband transitions), it is unclear why the *fastest* change in the amount of this spectral weight occurs in the doping region from $x=0$ to $x=0.2$, the region of *slowest* change in the position of the MIR absorption peak $\hbar\omega_{\text{max}}$, associated with the electronic gap energy and, therefore, with the band structure itself. Also, the first interband absorption peak above 2 eV can be observed at all doping concentrations,^{1,2} including those where $\lambda \approx 0$ and therefore all of the chemically doped electrons are accounted for by the MIR absorption. We consider this behavior an indicator that it is unlikely that the missing spectral weight is associated with high-order interband transitions.

Another way to account for the spectral weight distribution is through incoherent processes. As we have noted before, a number of publications appear to support the real-

space electron-pairing (small bipolaron or local CDW) model for BKBO. This model is different from the conventional CDW model in that bipolaron motion is incoherent due to severe localization of the electron pairs. We will examine the small bipolaron model next.

A small bipolaron (SBP) consists of two charge carriers strongly localized on a single site by their own short-range interaction with the lattice, taken together with the lattice displacement pattern caused by the interaction. Although a small bipolaron can be formed with a pair of holes as well as a pair of electrons, in the following by a small bipolaron we will mean a pair of electrons. As a result of the electron-lattice interaction a potential well of depth $-4E_b$ is formed, where E_b is the small-polaron binding energy.¹⁷ The ground-state energy of a SBP is, however, increased by the on-site Coulomb interaction energy U , a result of two electrons being on the same site. A small polaron is similar to a small bipolaron but contains only one electron.¹⁷ A single SBP is stable with respect to decay into two small polarons if the Coulomb energy U satisfies the condition $U < 2E_b$.¹⁷

We note that the bipolaronic model implies a doubling of the unit cell by a lattice modulation similar to what is observed experimentally in the undoped BaBiO₃.^{4,5} In analogy with small polarons,¹⁸ there is a strong repulsive interaction between two neighboring SBP's in BKBO as they disturb each other's pattern of oxygen ion displacements, thus raising the total energy. The interaction becomes weaker as the average distance between SBP's is increased. BaBiO₃ has one electron per formula unit and therefore the number of SBP's is half the number of Bi ions. As a result, individual SBP's are situated close to each other and the energy of interaction between SBP's is an important part of the total energy. Using a magnetic analog of this system it can be shown⁸ that, taking the interaction into account, the lowest energy is given by an antiferromagnetic-type configuration such as the one shown in Fig. 3. There are two interleaving fcc sublattices in this configuration: bipolaronic ($\text{Bi}^{3+} = \text{Bi}^{5+} + 2e^-$) sublattice *A* and empty (Bi^{5+}) sublattice *B*. The Bi^{5+} sites are strongly screened by overlap from the oxygens so that no site is strongly charged.¹⁹

A bipolaron can be excited in two ways. In the first scenario the pair of electrons associated with a bipolaron is excited to a neighboring Bi^{5+} site as a whole (two-particle excitation). This gives a peak in the corresponding absorption spectrum at $\hbar\omega_2 = 8E_b + 2\Delta$,²⁰ where by Δ we denote the difference in energy between the two sublattices due to bipolaron-bipolaron interaction. The second scenario involves pair breaking with excitation of a single electron (single-particle excitation). This gives an absorption peak at $\hbar\omega_1 = 4E_b - U + \Delta$.²⁰ The condition for formation of a single small bipolaron, $U < 2E_b$, is relaxed to a condition of stability of a bipolaron with respect to decay into one small polaron on sublattice *A* and one on sublattice *B*, $U < 2E_b + \Delta$. In fact, if $2E_b < U < 2E_b + \Delta$, a lattice of small bipolarons may form, although formation of *individual* small bipolarons is not energetically favorable. The peak frequency of the absorption band corresponding to the one-particle excitations, $\hbar\omega_1$, is always smaller than that corresponding to the two-particle excitations, $\hbar\omega_2$. The two processes can in general coexist, giving two peaks in the corresponding optical

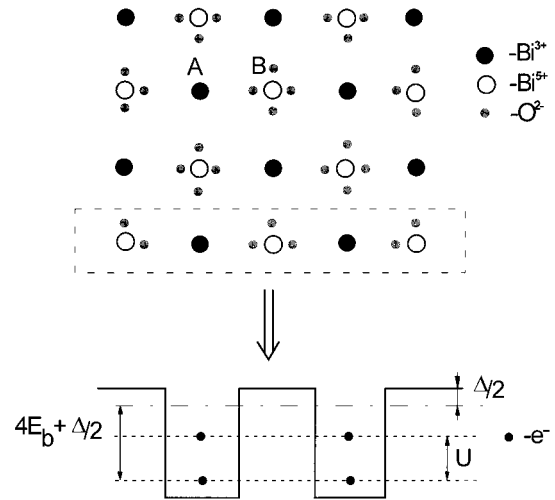


FIG. 3. The antiferromagnetic-type (bi)polaronic lattice. The (bi)polaronic sublattice is the sublattice *A*; the empty sublattice is the sublattice *B*. The lower part of the diagram shows schematically the energy configuration for one $\text{Bi}^{5+}-\text{Bi}^{3+}$ row with parameters discussed in the text. Polaronic lattice, at doping $x=0.5$, will look similar but each site in the sublattice *A* will contain only one electron.

conductivity. The spectral weight under both peaks must correspond to the total number of chemically doped carriers (or double the number of bipolarons) in a system. Therefore, the bipolaronic model can in principle provide an explanation for the fact that the spectral weight under the low-energy peak in nonmetallic BKBO is too small—the rest of the spectral weight may be contained in the absorption peak corresponding to the two-particle excitation process.

One difficulty arises here. It has been shown²¹ that the exponential terms in the expressions describing intensities (and spectral weights) of the absorption peaks corresponding to the two- and single-particle excitations are comparable. However, the SBP absorption intensity involves a preexponential factor, proportional to t_2^2 for the two-particle excitations and to t_1^2 for the single-particle excitations, where t_2 is a two-electron transfer energy (of order of an exchange energy) and t_1 is a one-electron transfer energy. The value of t_2 is usually smaller than t_1 and, therefore, at least for a dc motion of a single bipolaron by temperature-assisted hops in a periodic crystal potential, the single-particle excitation mechanism is thought to be more favorable¹⁸ so that the lower-energy (single-particle) absorption peak is supposed to be more intense. The experimental situation, at least for undoped BaBiO₃, is just the reverse: The low-frequency absorption peak contains just about 1/3 of the total spectral weight. However, the transfer energies for the thermal bipolaronic dc motion and the bipolaronic optical absorption may be different as they strongly depend on the atomic displacements.²⁰ In the case of dc motion one is interested in the transfer energy of thermally equilibrated carriers. In the case of optical absorption one is concerned with the transfer energy of a carrier at the coincidence event between energies of initial and final electronic states. Also, imperfections in the bipolaronic lattice, such as singly occupied sites, can give their own contribution to the optical conductivity through such processes as, for example, a hop of an electron from a

doubly occupied site to the singly occupied site. The energy required by such processes may be smaller or larger than the energy of the main single-particle excitation process, $\hbar\omega_1 = 4E_b - U + \Delta$, depending on the relation between E_b and Δ . Detailed perturbation theory calculations (including terms up to t_1^4) for a lattice of bipolarons would be helpful in understanding the optical transition probabilities and, therefore, the exact conductivity spectral weight distribution expected for this system.

Doping with potassium destroys bipolarons. When x is small, substituting K^+ for Ba^{2+} has the effect of taking one electron from a pair on an adjacent Bi^{3+} site. The electron that is left is, however, still localized on the Bi site in a potential well created by the surrounding bipolaronic lattice. At the same time, destroying a pair decreases the local energy difference Δ between B and A sublattices, making the surrounding electron pairs less stable and decreasing the bipolaronic hopping energy. Therefore, the frequency of the one-particle excitation peak in the optical conductivity will be reduced. Also, the spectral weight will shift to lower frequencies as there are fewer possibilities to excite a pair as a whole—there are fewer pairs. When doping is large enough so that the bipolaron coordination number z is smaller than a certain critical value z_c and $U > 2E_b + \Delta$, a first-order phase transition with discontinuous reduction of electron pairs will occur. However, the remaining electrons still strongly interact with the lattice so that in the hypothetical case where the transition occurs at $x_c = 0.5$ (and there are no remaining bipolaronic islands) they would arrange themselves in a *polaronic* lattice similar to that shown in Fig. 3 for *bipolarons*. However, if the transition occurs at $x_c < 0.5$, there are too many electrons left to form the antiferromagnetic-type lattice of Fig. 3. The extra $(0.5 - x_c)$ electrons have no place in the (now polaronic) sublattice A since the Coulomb repulsion U is too large to form a bipolaron. On the other hand, if they try to form polarons on the sublattice B , they disturb the atomic displacement patterns of neighboring polarons on sublattice A , reducing their stability and possibly releasing some of the localized carriers. Therefore, if $x_c < 0.5$, the electronic system may consist of dynamically occupied extended and localized states. This may explain the two optical absorption components: The MIR band represents electrons in the localized (experimental mean free path of about 6 Å) states and the Drude absorption is due to charge carriers in the extended states (mean free path of several hundred Å's). Experimentally, the spectral weight of the Drude electrons is about 6% of that of the MIR electrons at all metallic doping levels. However, it is difficult to assess if it is consistent with the model described above without detailed self-consistent calculations, in part because some fraction of the electrons may still be contained in the remaining bipolaronic islands. We note that our results do not exclude the possibility that the itinerant charge carriers are *large* bipolarons, which are bosons and may condense into a superfluidlike state at low temperatures.

It is interesting to compare the electronic gap in the BKBO system with the transition temperature from the “deformed” lattice configuration shown in Fig. 3 into the simple cubic lattice phase, T_{cubic} . We have plotted T_{cubic} , adopted from Ref. 7, by the crosses in Fig. 2(a) as a function of doping together with the peak energy of the MIR absorption.

The temperature scale has been chosen to normalize T_{cubic} to $\hbar\omega_{\text{max}}$ values. Also, we have put the zero of T_{cubic} near the lowest $\hbar\omega_{\text{max}}$ value corresponding to the lowest excitation energy of *paired* electrons, at x just below the IM transition boundary x_c . This minimal value of $\hbar\omega_{\text{max}}$ is equal to the excitation energy of a small polaron. Therefore, we effectively compare T_{cubic} with the reduction of electronic energy due to formation of *pairs*. The result is that the two quantities have surprisingly similar doping dependences suggesting an intimate relationship between the lattice vibrations and the dielectric properties of BKBO. However, the large difference in absolute values (about 20 times) still needs an explanation. Also, high-temperature dc transport measurements would be useful to determine the properties of the high-temperature phase of undoped $BaBiO_3$, in particular to determine if it is actually metallic.

Although it has been shown a number of times^{22,23} that the superconducting properties of metallic BKBO are closely related to those of the BCS model, results of a number of experiments indicate that the usual Fröhlich electron-phonon interaction is not strong enough to obtain $T_c \approx 31$ K.^{22–26} It was concluded that, although the mechanism of superconductivity in BKBO is probably BCS, an electron-electron interaction is not mediated by phonons in the usual way.²² We note in this respect that electrons, occupying the extended states in the system described above, may be prone to a relatively strong electron-electron interaction due to the polarizability of the localized states. It has been shown that high values of T_c can be achieved in a BCS model with such an interaction.²⁷

The optical conductivity for the metallic samples just above T_c and at $T = T_c/3$ is plotted in Fig. 4 at three different doping levels. The MIR absorption component is an almost flat background in this frequency range and has about the same value for all doping levels presented. The metallic BKBO is frequently thought to be an “overdoped” system,²⁵ that is, both a decrease of T_c and an improvement of the metallic properties are thought to be connected to an increase of the total density of metallic carriers. However, we did not observe a significant increase in the density of normal-state metallic (Drude) electrons with increasing x from $x = 0.38$ to $x = 0.46$, while low-temperature dc conductivity increased more than twice and T_c fell by 30%. The increase in the dc conductivity value with doping is mainly due to the decrease in the *scattering rate* $1/\tau$. The normal-state $1/\tau$ values of the Drude absorption at different x were determined from a fit to a two-component model similar to that used by us before²⁶ and is shown on the horizontal axis for the three doping levels. The simultaneous reduction of T_c and the scattering rate with increasing x in the metallic regime suggests that $1/\tau$ may include scattering of free carriers on bosonic excitations that mediate the superconducting pairing at low temperatures.

The low-frequency depression of $\sigma_1(\omega)$ at $T < T_c$ is due to the formation of the superfluid. We can roughly estimate the position of the superconducting gap $2\Delta_s$ as shown in Fig. 4 by arrows in all three panels. The gap energy decreases with decreasing T_c , keeping the ratio $2\Delta_s/k_B T_c = 4.2 \pm 0.3$ constant. The spectral weight that disappears in the superconducting state is contained in a δ peak at zero frequency and represents carriers that have condensed into the super-

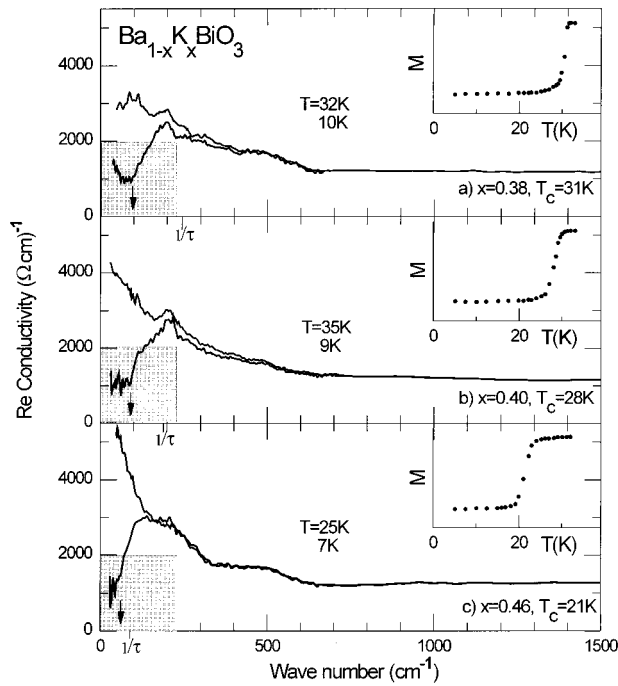


FIG. 4. The optical conductivity of the three metallic samples BKBO in the superconducting and the normal states. The results of magnetization measurements are shown on the insets. The scattering rate values $1/\tau$ in the normal state are shown on the frequency axis for all three samples. The shaded squares represent the spectral weight of the superconducting carriers. The London penetration depth λ_L is inversely proportional to the side of the square. The position of the superconducting gap energy $2\Delta_s$ is shown by the arrows.

fluid. Therefore the “missing” spectral weight is the spectral weight of the superconducting carriers and we can use it to estimate the London penetration depth value λ_L . We have performed the necessary calculations and the result is that within our error range λ_L has the same value $3750 \pm 100 \text{ \AA}$ at all doping levels, despite different T_c 's.²⁸ To make it more graphic we have drawn squares of areas equal to the spectral

weight “missing” in the superconducting state for all three doping levels. The sides of the squares are inversely proportional to λ_L and one can see that they are equal for all three samples. The areas themselves are proportional to the density of the superconducting carriers. Although the physical reasons for the insensitivity of λ_L to the doping level are not clear, one can see that there are two factors contributing to it: a decreasing superconducting gap value and a decreasing scattering rate. While a decrease in the scattering rate tends to pile up more conductivity below the superconducting gap energy in the normal state, which increases the number of carriers that condense into a superfluid at $T < T_c$, a decrease of the superconducting gap value tends to compensate for this.

In conclusion we have shown that the anomalous doping dependence of the distribution of the optical conductivity spectral weight in the BKBO system cannot be explained within the framework of a coherent-transport model with well-defined energy bands. This naturally leads to a local CDW, or bipolaronic, model. We have shown that this model can, at least qualitatively, explain some of the physical properties of the BKBO system, including the IM transition. However, we strongly emphasize that only more rigorous calculations than those presented in this work can provide the final answer. Experimentally, the IM transition at $x = x_c$ is associated with the appearance of the narrow free-carrier-like Drude absorption peak in the optical conductivity spectra. As the doping level increases in the metallic phase the width of the Drude peak decreases, increasing the dc conductivity value. At the same time the density of free carriers represented by the Drude absorption, as well as the London penetration depth value λ_L at $T = T_c/3$, do not change significantly with doping. The superconducting gap value Δ_s scales with T_c in a rough proportion $2\Delta_s/k_B T_c = 4.2 \pm 0.3$.

We would like to thank David Emin for many helpful discussions. This research was supported in part by the National Science and Engineering Research Council of Canada and by the Canadian Institute for Advanced Research. Research at the University of Illinois at Urbana-Champaign was sponsored by Contract No. NSF DMR 91-20000.

¹M.A. Karlow, S.L. Cooper, A.L. Kotz, M.V. Klein, P.D. Han, and D.A. Payne, Phys. Rev. B, **48**, 6499 (1993).

²S.N. Blanton, R.T. Collins, K.H. Kelleher, L.D. Rotter, Z. Schlesinger, D.G. Hinks, and Z. Zheng, Phys. Rev. B **47**, 996 (1993).

³P.D. Han, L. Chang, and D.A. Payne, J. Cryst. Growth **128**, 798 (1993).

⁴Shiyou Pei, J.D. Jorgensen, B. Dabrowski, D.G. Hinks, D.R. Richards, A.W. Mitchell, J.M. Newsam, S.K. Sinha, D. Vaknin, and A.J. Jacobson, Phys. Rev. B **41**, 4126 (1990).

⁵D.E. Cox and A.W. Sleight, Acta Crystallogr. Sect. B **35**, 1 (1979).

⁶L.F. Mattheiss and D.R. Hamann, Phys. Rev. B **28**, 4227 (1983).

⁷K. Takegahara, J. Electron Spectrosc. Relat. Phenom. **66**, 303 (1994).

⁸T.M. Rice and L. Sneddon, Phys. Rev. Lett. **47**, 689 (1981).

⁹S. Sugai, Y. Enomoto, and T. Murakami, Solid State Commun. **72**, 1193 (1989).

¹⁰A.V. Puchkov, T. Timusk, M.A. Karlow, S.L. Cooper, P.D. Han, and D.A. Payne, Phys. Rev. B **52**, R9855 (1995).

¹¹Y.Y. Wang, V.P. Dravid, N. Bulut, P.D. Han, M.V. Klein, S.E. Schnatterly, and F.C. Zhang, Phys. Rev. Lett. **75**, 2546 (1995).

¹²S. Tajima, S. Ucida, A. Masaki, H. Takagi, K. Kitazawa, S. Tanaka, and A. Katsui, Phys. Rev. B **35**, 696 (1987).

¹³The total optical conductivity in the metallic phase of BKBO can be fitted equally well by a sum of the MIR absorption band, modeled by an oscillator centered anywhere from 0 to 2000 cm^{-1} , and a Drude absorption band.

¹⁴D.Y. Smith, in *Handbook of Optical Constants of Solids*, edited by Edward D. Palik (Academic Press, London, 1985), pp. 35–64.

¹⁵P.B. Allen, Phys. Rev. B **3**, 305 (1971).

- ¹⁶Ivan Bosovic, J.H. Kim, J.S. Harris, Jr., E.S. Hellman, E.H. Hartford, and P.K. Chan, *Phys. Rev. B* **46**, 1182 (1992).
- ¹⁷David Emin, *Phys. Rev. B* **48**, 13 691 (1993).
- ¹⁸David Emin, *Phys. Today* **35**(6), 34 (1982).
- ¹⁹Nevill Mott, *Supercond. Sci. Technol.* **4**, S59 (1991).
- ²⁰David Emin, *Phys. Rev. B* **53**, 1260 (1996); (private communication).
- ²¹V.V. Bryksin and V.S. Voloshin, *Sov. Phys. Solid State* **26**, 1429 (1984).
- ²²F. Marsiglio, J.P. Carbotte, A.V. Puchkov, and T. Timusk, *Phys. Rev. B* **53**, 9433 (1996).
- ²³For tunneling measurements see, for example, F. Sharifi, A. Pargellis, R.C. Dynes, B. Miller, E.S. Hellman, J. Rosamilia, and E.H. Hartford, Jr., *Phys. Rev. B* **44**, 12 521 (1991).
- ²⁴F. Marsiglio and J.P. Carbotte, *Phys. Rev. B* **52**, 16 192 (1995); J.E. Graebner, L.F. Schneemeyer, and J.K. Thomas, *ibid.* **39**, 9682 (1989).
- ²⁵B. Batlogg, R.J. Cava, L.W. Rupp, Jr., A.M. Mjuscce, J.J. Krajewski, J.P. Remeika, W.F. Peck, Jr., A.S. Cooper, and G.P. Espinosa, *Phys. Rev. Lett.* **61**, 1670 (1988).
- ²⁶A.V. Puchkov, T. Timusk, W.D. Mosley, and R.N. Shelton, *Phys. Rev. B* **50**, 4144 (1995).
- ²⁷See, for example, Vladimir Z. Kresin and Stuart A. Wolf, *Fundamentals of Superconductivity* (Plenum Press, New York, 1990). Also A.J. Heeger and G. Yu, *Phys. Rev. B* **48**, 6492 (1993).
- ²⁸The value of λ_L obtained by us previously (Ref. 26) was somewhat overestimated due to lack of reliable high-frequency reflectivity data. Using ellipsometric results in combination with the reflectivity data makes λ_L more reliable.